IOP Conference Series: Earth and Environmental Science

PAPER • **OPEN ACCESS**

Baroclinic low-level jets in Arctic marine cold-air outbreaks

To cite this article: D G Chechin and C Lüpkes 2019 *IOP Conf. Ser.: Earth Environ. Sci.* **231** 012011

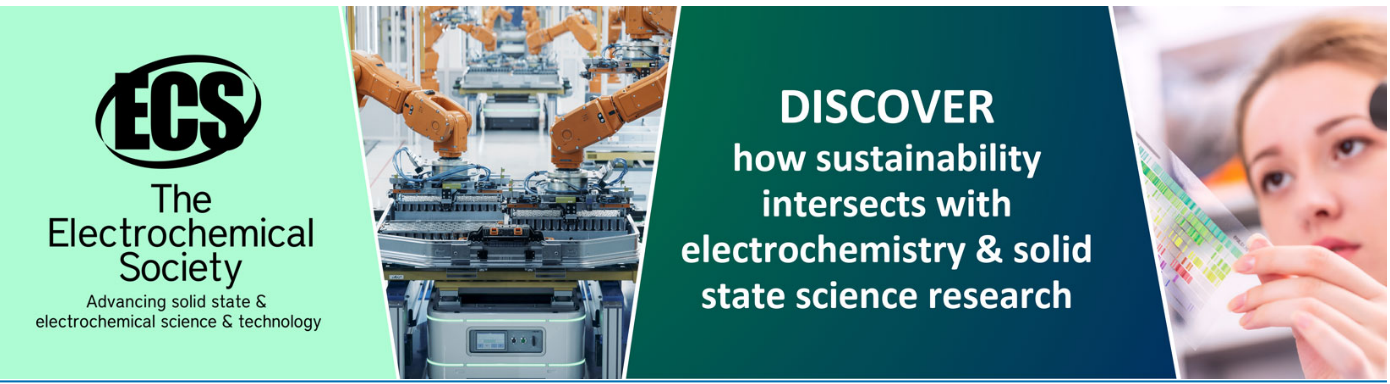

IOP Conf. Series: Earth and Environmental Science 231 (2019) 012011 doi:10.1088/1755-1315/231/1/012011

Baroclinic low-level jets in Arctic marine cold-air outbreaks

D G Chechin[1,2], **C Lüpkes**[1]

[1] Alfred-Wegener-Institute Helmholtz Centre for Polar and Marine Research, Bremerhaven, Germany

[2] A.M. Obukhov Institute of Atmospheric Physics of the Russian Academy of Sciences, Moscow, Russia

E-mail: chechin@ifaran.ru

Abstract. An analytical model describing the evolution of a convective atmospheric boundary layer in marine cold-air outbreaks in the Arctic is presented. The novelty of the model is a detailed description of the baroclinicity associated with the boundary-layer growth and heating. Ekman friction is also taken into account. Thereby, the model describes the evolution of mixed-layer wind components over the ocean. It is shown theoretically that baroclinicity leads either to deceleration or to acceleration of the flow over the ocean, which depends on the direction of the large-scale flow relative to the orientation of the ice edge. Acceleration of the flow leads to a formation of a low-level jet strongly affecting the surface fluxes of heat and momentum. Baroclinicity and the magnitude of the low-level jet are strongest close to the ice edge being proportional to the ocean-ice temperature difference and decays further downwind. Horizontal decay of the low-level jet strength is governed by the airmass transformation length scale which is estimated to be in the order of 500-1000 km for typical cold-air outbreaks. The model solutions are shown to be in good agreement with aircraft observations over the Fram Strait and results of a numerical nonhydrostatic model.

1. Introduction

Cold-air outbreaks (CAOs) represent the advection of a cold Arctic airmass over a relatively warm open ocean. The key feature of CAOs is a large heat loss of the ocean due to an extremely high surface turbulent heat flux. This shapes their role in the climate system. Namely, CAOs strongly influence i) the water-mass modification and ii) the meridional heat exchange in the atmosphere.

The magnitude of the surface heat flux in CAOs is primarily governed by a large temperature difference between the cold airmass and the ocean, but is also modulated by wind speed. Especially intense during CAOs can be mesoscale circulations such as polar mesocyclones, low-level fronts, orographic and baroclinic jets. The latter are in the focus of this study.

Earlier studies [1, 2, 3] hypothesized that the atmospheric boundary-layer heating during CAOs can lead to acceleration of the flow and formation of low-level jets. A systematic study of this phenomena has been carried out in [4, 5] and [6]. In the latter paper, we proposed a simple mixed-layer model describing the atmospheric boundary-layer evolution during CAOs, associated baroclinicity and its impact on wind speed. The model was evaluated by comparison with aircraft observations over the Fram Strait in the Arctic and with results of a more complete three-dimensional nonhydrostatic model NH3D. Here, we summarize the results of [6] and also use simple schematics to better illustrate the effect of baroclinicity on wind speed in CAOs.

2. Analytical model

The analytical model is based on an idealized mixed-layer representation of the vertical profiles of potential temperature and horizontal wind components in the convective atmospheric boundary layer (ABL) over the ocean downwind the ice edge (Fig. 1a). The steady-state assumption is used. The model consists of prognostic equations for the mixed-layer potential temperature θ_m, temperature jump at the boundary layer top $\Delta\theta$ and the mixed-layer height z_i, as well as of the diagnostic equations for the mixed-layer horizontal wind components u_m and v_m. The latter equations represent a so-called geotriptic (or Ekman) balance, i.e. the balance between the horizontal pressure gradient force, Coriolis force and friction.

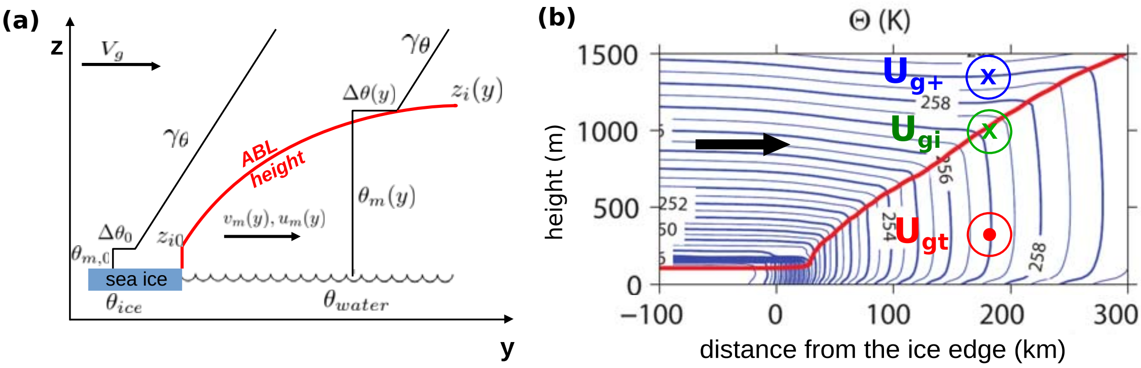

Figure 1. (a): Idealized mixed-layer representation of the ABL structure in marine cold-air outbreaks. (b): Vertical cross section of potential temperature in CAO and baroclinic components of the along-ice component of the geostrophic wind: U_{gt} points out of the figure; U_{gi} and U_{g+} point into the figure.

As discussed in Chechin et al. [6], it is possible to solve the prognostic equations for θ_m, z_i and $\Delta\theta$ independently from the momentum equations. The solution closely follows the one presented by Venkatram [7]. As a result, one obtains a prognostic equation for the normalized mixed-layer potential temperature $\overline{\theta_m}$ as function of the normalized distance from the ice edge $\overline{y}$, namely

$$\ln(1-\overline{\theta_\mathrm{m}})+\overline{\theta_\mathrm{m}} = -\mathrm{C_1}\overline{\mathrm{y}}+\mathrm{C_2}\ , \tag{1}$$

where C_1 and C_2 are constants consisting of external parameters. The normalized ABL height $\overline{z_i}$ and temperature jump $\overline{\Delta\theta}$ are linearly related to $\overline{\theta_m}$.

The solution, given by Eq. 1, is further used to obtain relations describing baroclinic components of the geostrophic wind in the ABL as functions of distance from the ice edge. After that, the known geostrophic wind speed and z_i are used in the Ekman balance equations to find u_m and v_m.

3. Mixed-layer geostrophic wind

One of the key parts of the model is a representation of the along-ice mixed-layer geostrophic wind component u_{gm} as a sum

$$u_{gm} = U_g + U_{gt} + U_{gi} + U_{g+}\ , \tag{2}$$

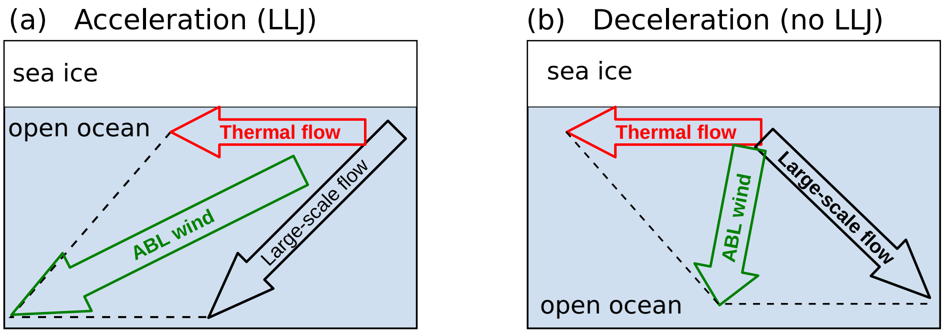

Figure 2. Schematic representation of the vector sum of the large-scale geostrophic wind and the baroclinic thermal component: case (a) represents acceleration of the flow in the ABL due to baroclinicity; case (b) represents deceleration.

where U_g is the large-scale barotropic component of the geostrophic wind, and U_{gt}, U_{gi} and U_{g+} are the baroclinic components associated with the boundary-layer heating and growth (Fig. 1b). The first term U_{gt} is related to the horizontal temperature gradient in the ABL and is given by

$$U_{gt} = \frac{g z_i}{2 f \theta_m} \frac{\partial \theta_m}{\partial y} \ , \tag{3}$$

where g is the acceleration due to gravity, f - Coriolis parameter. The second baroclinic term U_{gi} is due to sloping of the inversion at the ABL top. The latter is maintained by the entrainment. It can be shown [6], that U_{gi} is a fraction of U_{gt} and amounts to about $0.3U_{gt}$ depending on the entrainment rate . The third baroclinic term U_{g+} is related to the horizontal temperature gradient above the ABL, which forms as a result of the mass adjustment above the ABL. Based on results of the nonhydrostatic model NH3D, Chechin et al. [6] concluded that at a distance larger than about 100 km downwind the ice edge U_{g+} is also proportional to U_{gt} and amounts to about 30% of the U_{gt} value for typical CAO conditions. Thus, U_{gt} is the dominant baroclinic term, which determines the effect of baroclinicity on the ABL wind speed. The terms U_{gi} and U_{g+} have opposite sign representing thermal counterflow above the ABL, which in the opposite direction to the thermal flow in the ABL, as shown in Fig. 1b.

The baroclinic thermal flow in the ABL is directed parallel to the ice edge with cold on the right. Thus, the absolute value of the vector sum of the baroclinic thermal wind in the ABL and the large-scale geostrophic wind can either be larger or smaller than the absolute value of the large-scale geostrophic wind, as shown in Fig. 2. This leads either to acceleration and a low-level jet formation or deceleration of the ABL wind depending on the angle between the large-scale wind and the orientation of the ice edge. This phenomena was studied using idealized numerical experiments in [4] and using reanalysis and satellite data for several CAOs in [5].

4. Comparison to aircraft observations

In this section, analytical solutions are compared to aircraft observations over the Fram Strait performed by the Alfred Wegener Institute, Bremerhaven (Germany). The observations from six cases of cold-air outbreaks are used. Figure 3 shows the normalized mixed-layer potential temperature, height and the baroclinic component $\overline{U_{gt}}$ as functions of normalized distance from the ice edge together with analytical solutions. It can be seen, that the ABL temperature and height collapse quite well and closely follow the analytical solution. However, the ABL temperature is underestimated by the analytical solution probably due to neglect of condensation. The values of $\overline{U_{gt}}$ demonstrate larger scatter around the analytical curve, but nevertheless, the agreement is reasonable.

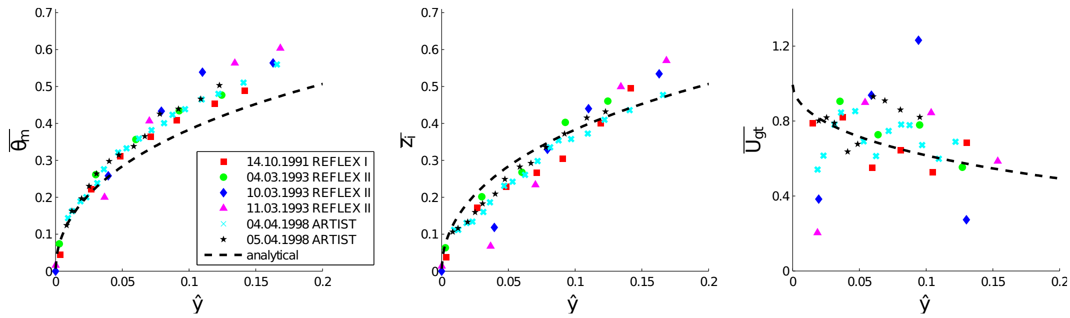

Figure 3. Normalized mixed-layer potential temperature $\overline{\theta_m}$, ABL height $\overline{z_i}$ and baroclinic component $\overline{U_{gt}}$ as functions of distance from the ice edge $\hat{y} = C_1\overline{y} - C_2$ based on the aircraft observations from several campaigns of Alfred Wegener Institute, Bremerhaven (Germany); blue dashed lines represent the analtical solutions. The figure is adopted from [6].

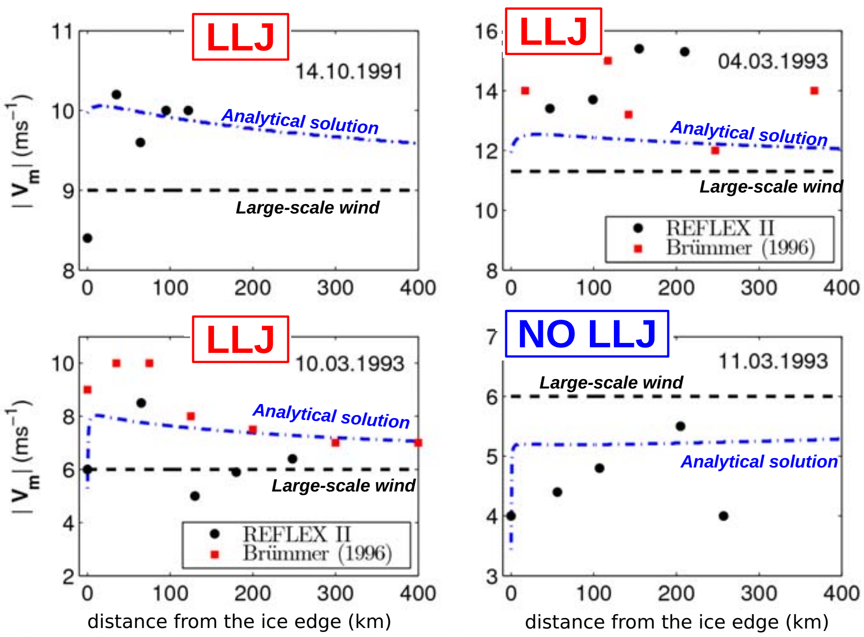

Figure 4. The observed mixed-layer wind speed and the large-scale geostrophic wind (black dashed line) as functions of distance from the ice edge; blue dashed line represent the analytical solution. The figure is adopted from [6].

The model also predicts well the acceleration and deceleration of the flow in the ABL. Figure 4 shows the observed mixed-layer wind speed and the large-scale gepstrophic wind (black dashed line). It can be seen that in three cases (14.10.1991, 04.03.1993 and 10.03.1993) where the acceleration of the flow was observed the model also produced acceleration. On those days the flow over the Fram Strait was from the north-east crossing the ice edge oriented in the west-east direction. As shown in Fig. 2a, a low-level jet forms for this flow direction. On 11.03.1993, the large-scale flow was from north-west and deceleration of the flow was observed. Two more cases are not shown in Fig. 4 because the large-scale flow was quite strong (15-17 ms^{-1}) and the relative effect of baroclinicity could not be identified both in the observations and was also very small in the analytical solutions. Finally, Fig. 3-4 show that baroclinicity and its effect on wind speed decrease downwind the ice edge. As shown analytically in [6] the decay of baroclinicity with distance from the ice edge is governed by the airmass transformation scale. An analytical expression was obtained for the latter scale. It shows that this scale is proportional to the temperature difference between ocean and sea ice and varies in the range 500-1000 km for typical Arctic CAOs.

To conclude, the proposed model shows good qualitative and quantitative agreement with observations. It highlights the effect of baroclinicity on wind speed leading to the presence or absence of a low-level jet. The model describes the sensitivity of the low-level jet strength and horizontal extent to the external parameters, such as the ocean-ice temperature difference, direction of the large-scale flow, temperature lapse rate above the ABL. The model can be used as an analytical tool to interpret observations and results of numerical simulations.

Acknowledgments
The study was supported by German Research Foundation (DFG, Deutsche Forschungsgemeinschaft) grant within the Transregional Collaborative Research Center (TR 172) “Arctic Amplification: Climate Relevant Atmospheric and SurfaCe Processes, and Feedback Mechanisms (AC)3” and the Russian Foundation for Basic Research Grant 18-05-80065.

References

[1] Overland J E, Reynolds R M and Pease C H 1983 *J. Geophys. Res.* **88** 2836–40
[2] Yuen C-W and Young J A 1986 *J. Atmos. Sci.* **43(24)** 3089–3108
[3] Brümmer B 1996 *Boundary-Layer Meteorol.* **80** 109–25
[4] Chechin D G, Lüpkes C, Repina I A, Gryanik V M 2013 *J. Geophys. Res* **118** 8787–8813
[5] Chechin D G, Zabolotskih E V, Repina I A and Chapron B 2015 *Izv. Atmos. Ocean. Phys.* **51(2)** 127–37
[6] Chechin D G and Lüpkes C 2017 *Boundary-Layer Meteorol.* **162(1)** 91–116
[7] Venkatram A 1977 *Boundary-Layer Meteorol.* **11(4)** 419–37